

SYNTHESIS, STRUCTURE, AND ELECTRIC PROPERTIES OF $\text{Li}_{1+x}\text{Sc}_x\text{Zr}_{2-x}(\text{PO}_4)_3$ ($x = 0.1, 0.2, 0.3$) CERAMICS

T. Šalkus^a, A. Dindune^b, Z. Kanepe^b, J. Ronis^b, A. Kežionis^a, and A.F. Orliukas^a

^a Faculty of Physics, Vilnius University, Saulėtekio 9, LT-10222 Vilnius, Lithuania

E-mail: tomas.salkus@ff.vu.lt

^b Institute of Inorganic Chemistry at the Riga Technical University, Miera 34, LV-2169 Salaspils, Latvia

Received 5 July 2006

The solid electrolyte $\text{Li}_{1+x}\text{Sc}_x\text{Zr}_{2-x}(\text{PO}_4)_3$ (where $x = 0.1, 0.2, 0.3$) compounds were synthesized by a solid state reaction and studied by X-ray diffraction at room temperature. At room temperature the investigated compounds belong to rhombohedral symmetry (space group $R\bar{3}c$) with six formula units in the lattice. The ceramic samples were investigated by complex impedance spectroscopy in the frequency range from 10^6 to $1.2 \cdot 10^9$ Hz at temperatures ranging from 300 to 600 K. Two regions of relaxation dispersion were found. The dispersions are related to the fast Li^+ ion transport in the grains and grain boundaries of ceramics. Variation of the stoichiometric parameter affects the density of the ceramics, the values of total and grain conductivity, their activation energies, and frequency of the relaxation processes in the materials. The increase of parameter x leads to the increase of values of total and grain conductivities, dielectric permittivity, and dielectric losses of the ceramics.

Keywords: ionic conductivity, permittivity, relaxation dispersion, synthesis, ceramic, sintering

PACS: 61.10.Nz, 66.30.Hs, 81.05.Je, 82.45.Yz

1. Introduction

Lithium ion conductors are especially promising as solid electrolytes for a number of reasons. The compounds with fast Li ion transport are attractive materials for development of high energy batteries [1, 2] and sensitive CO_2 sensors [3, 4]. The compounds with formula $\text{LiM}_2(\text{PO}_4)_3$ (where $M = \text{Ge}, \text{Zr}, \text{Ti}$) belong to a group of crystals with NASICON-type network structure and are extensively studied because of their high ionic conductivity and chemical stability [5–7]. The ionic conductivity of the system is greatly increased when Zr^{4+} in $\text{LiZr}_2(\text{PO}_4)_3$ is replaced by a smaller Ti^{4+} ion, since the tunnels in $\text{LiTi}_2(\text{PO}_4)_3$ are more suitable in size for the Li^+ ion migration [5]. It is known [6, 8, 9] that partial substitution of Ti^{4+} by Sc^{3+} , In^{3+} , Cr^{3+} ions in the NASICON-type structure of $\text{LiTi}_2(\text{PO}_4)_3$ compound causes an increase of the value of the Li ion conductivity σ of the substituted systems.

The substitution of Zr^{4+} by Ti^{4+} and trivalent ion Sc^{3+} in the $\text{LiZr}_2(\text{PO}_4)_3$ compound causes a drastic increase of σ at room temperature in comparison with the value of ionic conductivity of $\text{Li}_{1+x}\text{Zr}_{2-x}\text{Ti}_x(\text{PO}_4)_3$ compound. At room temperature the value of σ of $\text{Li}_{1.2}\text{Sc}_{0.6}\text{Zr}_{0.6}\text{Ti}_{1.6}(\text{PO}_4)_3$ compound was found to be

$1.2 \cdot 10^{-2}$ S/m and to increase with temperature, at having the activation energy $\Delta E = 0.33$ eV [5]. In the present work we are going to investigate the materials based on $\text{LiZr}_2(\text{PO}_4)_3$ compound.

The crystal structure of $\text{LiZr}_2(\text{PO}_4)_3$ depends on the technological conditions of preparation of the compound. The X-ray pattern of $\text{LiZr}_2(\text{PO}_4)_3$ prepared at 1323–1373 K greatly differs from rhombohedral and possibly corresponds to a triclinic cell [10]. At 1423–1473 K temperature sintered $\text{LiZr}_2(\text{PO}_4)_3$ pellets belong to rhombohedral symmetry (lattice parameters $a = 8.860$ Å and $c = 22.13$ Å). According to whether synthesis is carried out at a temperature of 1473 or 1173 K, two different phases are obtained [11]. The $\text{LiZr}_2(\text{PO}_4)_3$ compound prepared at 1473 K shows a NASICON-type structure and a monoclinic rhombohedral first order transition takes place at a temperature of about 313 K. $\text{LiZr}_2(\text{PO}_4)_3$ prepared at lower temperature (1173 K) exhibits the $\beta\text{-Fe}_2(\text{SO}_4)_3$ -type structure and a monoclinic–orthorhombic transformation takes place at 573 K temperature.

The authors of [12, 13] have reported that $\text{LiZr}_2(\text{PO}_4)_3$ samples heated at 1473 and 1373 K belong to a triclinic symmetry. For materials prepared at 1473 and 1173 K the values of ionic conductivity at

573 K temperature was found to be $\sigma = 1.2$ S/m and $\sigma = 5 \cdot 10^{-2}$ S/m respectively [11]. At room temperature the value of ionic conductivity of $\text{LiZr}_2(\text{PO}_4)_3$ is lower than 10^{-7} S/m.

In the present work we report the conditions for the synthesis of the $\text{Li}_{1+x}\text{Sc}_x\text{Zr}_{2-x}(\text{PO}_4)_3$ powder, sintering of the ceramic samples, and the results of our investigations of X-ray diffraction from the powder, as well as electrical properties of the ceramics in the frequency range from 10^6 to $1.2 \cdot 10^9$ Hz and in the temperature range from 300 to 600 K.

2. Experimental

The powder of $\text{Li}_{1+x}\text{Sc}_x\text{Zr}_{2-x}(\text{PO}_4)_3$ (where $x = 0.1, 0.2, 0.3$) was synthesized from a mixture of ZrO_2 (plasma synthesized nanodispersed powder), Li_2CO_3 (99.999%), Sc_2O_3 (99.99%), and $\text{NH}_4\text{H}_2\text{PO}_4$ (extra pure) by a solid state reaction. The stoichiometric mixture was heated for 6 h at a temperature $T = 723$ K, then milled in a planetary mill for 12 h. The obtained powder was heated for 2.5 h at 1173 K. After milling, the powder was heated for 2.5 h at $T = 1473$ K, then milled again and heated at $T = 1573$ K for 7 h. Finally, the mixture was milled and dried at 393 K temperature for 24 h. The millings were carried out in ethyl alcohol. Average grain size of the powder was found to be 1 μm . The structure parameters were obtained at room temperature from the X-ray powder diffraction patterns in the region $2\Theta = 6^\circ, \dots, 80^\circ$ with a step of 1°min^{-1} using $\text{Cu K}\alpha$ radiation. The powder was plasticized by polypropylenglycol 425 and uniaxially cold pressed at 300 MPa. The sintering of the samples was conducted in air at temperature $T = 1643$ K for 1 h. The measurements of complex conductivity $\tilde{\sigma} = \sigma' + i\sigma''$, complex impedance $\tilde{Z} = Z' + iZ''$, and complex dielectric permittivity $\tilde{\epsilon} = \epsilon' + i\epsilon''$ were performed in the temperature range from 300 to 600 K in a frequency range from 1 MHz to 1.2 GHz by a coaxial impedance spectrometer set-up [14]. All measurements were carried out in air.

3. Results and discussion

The results of the X-ray diffraction study have shown that $\text{Li}_{1+x}\text{Sc}_x\text{Zr}_{2-x}(\text{PO}_4)_3$ (where $x = 0.1, 0.2, 0.3$) powder is mainly a single phase material. The corresponding X-ray powder diffraction data are listed in Table 1.

The $\text{Li}_{1+x}\text{Sc}_x\text{Zr}_{2-x}(\text{PO}_4)_3$ compounds belong to the rhombohedral symmetry (space group $R\bar{3}c$) with six formula units in the lattice. The lattice parameters, unit

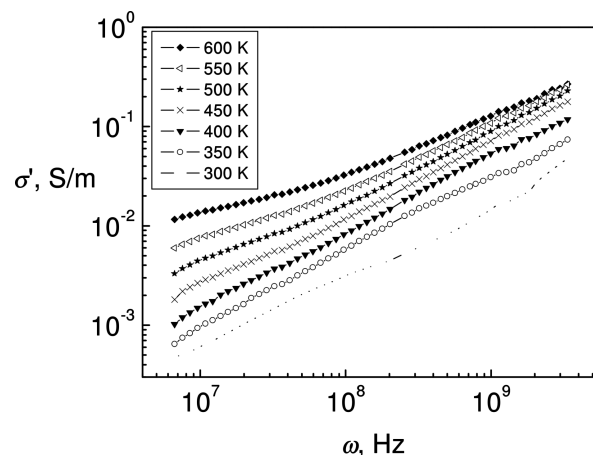


Fig. 1. Frequency dependences of the real part of conductivity of $\text{Li}_{1.2}\text{Sc}_{0.2}\text{Zr}_{1.8}(\text{PO}_4)_3$ ceramics at different temperatures.

cell volume V , and density $d_{\text{X-ray}}$ of the investigated compounds together with the data of $\text{LiZr}_2(\text{PO}_4)_3$ compound [15] are presented in Table 2.

The substitution of Zr^{4+} by Sc^{3+} in $\text{LiZr}_2(\text{PO}_4)_3$ causes a decrease of the lattice parameters of the $\text{Li}_{1+x}\text{Sc}_x\text{Zr}_{2-x}(\text{PO}_4)_3$ compound. The variations can be caused by the different values of ionic radii of Zr^{4+} and Sc^{3+} ions. The ionic radii of Zr^{4+} and Sc^{3+} are 0.8 Å [16] and 0.745 Å [17] respectively.

The densities of ceramics with $x = 0.1, 0.2$, and 0.3 were found to be 58%, 61%, and 66% of the theoretical densities of the respective compounds.

The impedance investigation of the ionic conductivity in the wide frequency and temperature ranges has an advantage because it allows one to separate the charge carrier transport processes in grains and in grain boundaries of the ceramics.

The characteristic frequency dependences of the real part of $\tilde{\sigma}$ for $\text{Li}_{1.2}\text{Sc}_{0.2}\text{Zr}_{1.8}(\text{PO}_4)_3$ ceramics at different temperatures are shown in Fig. 1. Two dispersion regions were found in σ' spectra for all the investigated samples. The high frequency part of the obtained spectra may be attributed to the relaxation in grains, while the lower frequency part corresponds to the grain boundary processes, like in the wide range of other solid electrolyte ceramics [18–21].

Both processes are thermally activated and dispersion regions shift toward higher frequencies with the increase of temperature. The characteristic complex impedance and complex conductivity plots of the ceramic samples at different temperatures are shown in Figs. 2 and 3. The temperature dependences of total (σ_t) and grain (σ_g) conductivities of $\text{Li}_{1+x}\text{Sc}_x\text{Zr}_{2-x}(\text{PO}_4)_3$ ceramics were derived from the complex plots of $\tilde{Z}(\omega)$ and $\tilde{\sigma}(\omega)$ (where $\omega = 2\pi f$) at different tem-

Table 1. X-ray powder diffraction data for $\text{Li}_{1+x}\text{Sc}_x\text{Zr}_{2-x}(\text{PO}_4)_3$ (where $x = 0.1, 0.2, 0.3$) compounds at room temperature.

$\text{Li}_{1.1}\text{Sc}_{0.1}\text{Zr}_{1.9}(\text{PO}_4)_3$				$\text{Li}_{1.2}\text{Sc}_{0.2}\text{Zr}_{1.8}(\text{PO}_4)_3$				$\text{Li}_{1.3}\text{Sc}_{0.3}\text{Zr}_{1.7}(\text{PO}_4)_3$			
$2\Theta, ^\circ$	$d, \text{\AA}$	hkl	$I/I_0, \%$	$2\Theta, ^\circ$	$d, \text{\AA}$	hkl	$I/I_0, \%$	$2\Theta, ^\circ$	$d, \text{\AA}$	hkl	$I/I_0, \%$
14.08	6.29	0 1 2	20	14.05	6.30	0 1 2	28	14.03	6.31	0 1 2	24
19.84	4.48	1 0 4	100	19.82	4.48	1 0 4	81	19.84	4.48	1 0 4	90
20.06	4.43	1 1 0	65	20.03	4.43	1 1 0	51	20.01	4.44	1 1 0	67
23.37	3.81	1 1 3	92	23.42	3.79	1 1 3	100	23.47	3.79	1 1 3	100
28.32	3.151	0 2 4	65	28.32	3.151	0 2 4	73	28.34	3.149	0 2 4	77
31.12	2.874	2 1 1	18	31.08	2.877	2 1 1	14	31.08	2.877	2 1 1	17
31.63	2.829	1 1 6	62	31.64	2.828	1 1 6	51	31.64	2.828	1 1 6	56
34.53	2.597	1 0 8	3	34.63	2.590	1 0 8	3	34.65	2.590	1 0 8	4
34.99	2.564	2 1 4; 3 0 0	42	35.02	2.562	3 0 0	44	35.00	2.564	3 0 0	51
40.25	2.241	2 0 8	7	40.27	2.394	2 0 8	6	40.33	2.236	2 0 8	6
42.08	2.147	1 1 9	6	42.16	2.143	1 1 9	4	42.20	2.141	1 1 9	6
42.60	2.122	2 2 3	10	42.67	2.119	2 2 3	6	42.67	2.119	2 2 3	6
43.08	2.100	3 0 6	4	43.05	2.101	3 0 6	3	43.24	2.092	3 1 2	4
43.28	2.090	3 1 2	5	43.27	2.091	3 1 2	4	45.44	1.9960	2 1 8	23
45.30	2.0018	2 1 8	23	45.40	1.9976	2 1 8	22	45.65	1.9873	3 1 4	14
45.70	1.9852	3 1 4	17	45.68	1.9860	3 1 4	17	47.60	1.9103	2 0 10	7
47.46	1.9156	2 0 10	9	47.56	1.9118	2 0 10	9	47.91	1.8987	2 2 6	18
47.90	1.8990	2 2 6	18	47.90	1.8990	2 2 6	15	48.04	1.8938	4 0 2	17
51.98	1.7592	4 0 5	21	51.80	1.7649	3 1 7	3	51.83	1.7639	3 1 7	5
53.88	1.7015	4 0 6	4	52.08	1.7560	2 1 10	17	52.12	1.7548	2 1 10	17
54.40	1.6865	3 1 8	12	54.03	1.6972	1 1 12	4	54.06	1.6963	1 1 12	4
54.80	1.6751	4 1 0	33	54.42	1.6859	3 1 8	10	54.46	1.6848	3 1 8	10
56.34	1.6329	4 1 3	4	54.80	1.6751	4 1 0	22	54.75	1.6765	4 1 0	28
58.53	1.5770	4 0 8	6	56.28	1.6345	4 1 3	3	56.30	1.6340	4 1 3	3
59.82	1.5460	1 0 14	6	58.60	1.5752	4 0 8	4	58.60	1.5752	4 0 8	4
60.32	1.5344	5 0 1	11	60.40	1.5325	5 0 1	9	60.02	1.5413	1 0 14	6
60.70	1.5257	4 1 6	9	60.72	1.5252	4 1 6	6	60.47	1.5309	3 1 10	11
62.80	1.4796	5 0 4	7	62.80	1.4796	5 0 4	6	60.70	1.5257	4 1 6	10
63.70	1.4609	3 1 11	5	64.32	1.4482	4 0 10	4	62.70	1.4817	5 0 4	7
64.26	1.4495	4 0 10	7	70.32	1.3387	5 1 4	6	63.96	1.4555	2 0 14	7
70.38	1.3377	5 1 4	6					64.10	1.4527	0 5 5	6
								64.34	1.4476	4 0 10	6
								70.32	1.3387	5 1 4	7

Table 2. Summary of X-ray diffraction results for $\text{Li}_{1+x}\text{Sc}_x\text{Zr}_{2-x}(\text{PO}_4)_3$ and host compounds at room temperature.

Compound	Lattice parameters		$V, \text{\AA}^3$	$d_{\text{X-ray}}, \text{g/cm}^3$
	$a, \text{\AA}$	$c, \text{\AA}$		
$\text{LiZr}_2(\text{PO}_4)_3$	8.8077	22.715	1526.05	3.10
$\text{Li}_{1.1}\text{Sc}_{0.1}\text{Zr}_{1.9}(\text{PO}_4)_3$	8.8613(31)	22.0968(155)	1502.65	3.12
$\text{Li}_{1.2}\text{Sc}_{0.2}\text{Zr}_{1.8}(\text{PO}_4)_3$	8.8703(23)	22.0492(76)	1502.44	3.09
$\text{Li}_{1.3}\text{Sc}_{0.3}\text{Zr}_{1.7}(\text{PO}_4)_3$	8.8727(24)	22.0199(67)	1501.27	3.07

Table 3. Results of measurements of σ_t , ΔE_t , σ_g , and ΔE_g for $\text{Li}_{1+x}\text{Sc}_x\text{Zr}_{2-x}(\text{PO}_4)_3$ ceramic samples with different stoichiometric parameter x .

Stoichiometric parameter x	$\sigma_t, \text{S/m}$	$\Delta E_t, \text{eV}$	$\sigma_g, \text{S/m}$	$\Delta E_g, \text{eV}$
	$T = 600 \text{ K}$		$T = 300 \text{ K}$	
0.1	0.00328	0.30	0.00149	0.30
0.2	0.0117	0.49	0.00184	0.29
0.3	0.0454	0.41	0.00338	0.28

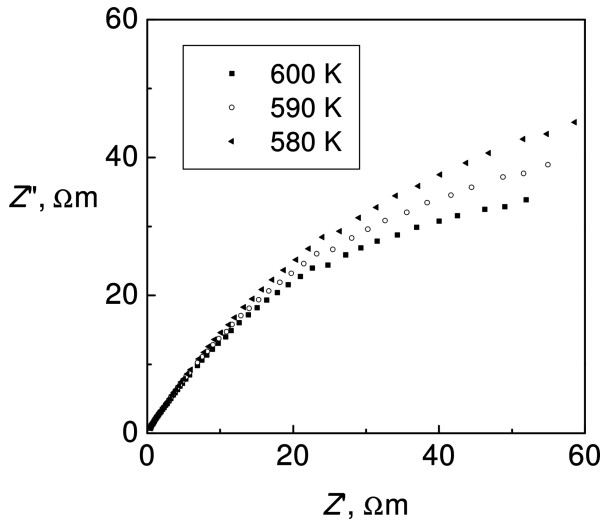


Fig. 2. Complex plane plots of conductivity of $\text{Li}_{1.2}\text{Sc}_{0.2}\text{Zr}_{1.8}(\text{PO}_4)_3$ ceramics at different temperatures.

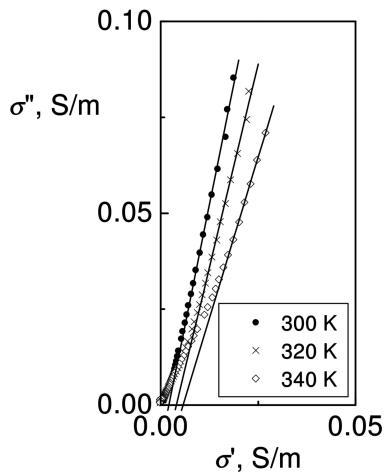


Fig. 3. Complex plane plots of impedance of $\text{Li}_{1.2}\text{Sc}_{0.2}\text{Zr}_{1.8}(\text{PO}_4)_3$ ceramics at different temperatures.

peratures. The temperature dependences of σ_t and σ_g of the ceramic samples are shown in Fig. 4. The activation energies of σ_t and σ_g were found from the slopes of the Arrhenius plots. The results of investigation of σ_t , σ_g , activation energy of total conductivity ΔE_t , and activation energy of grain conductivity ΔE_g for different x are summarized in Table 3.

The temperature dependences of dielectric permittivity ϵ' and dielectric losses $\tan \delta$ were investigated at the frequency of 1 GHz. This frequency is higher than Maxwell relaxation frequency $\omega_M = \sigma_g / (\epsilon' \epsilon_0)$ (where $\epsilon_0 = 8.85 \cdot 10^{-12}$ F/m is dielectric constant of the vacuum). At temperature $T = 350$ K the ω_M of the ceramics with $x = 0.1, 0.2, 0.3$ were found to be 130, 183, and 284 MHz, respectively. The temperature dependences of ϵ' and $\tan \delta$ of $\text{Li}_{1+x}\text{Sc}_x\text{Zr}_{2-x}(\text{PO}_4)_3$ ceramics with different x are shown in Figs. 5 and 6 respectively. At

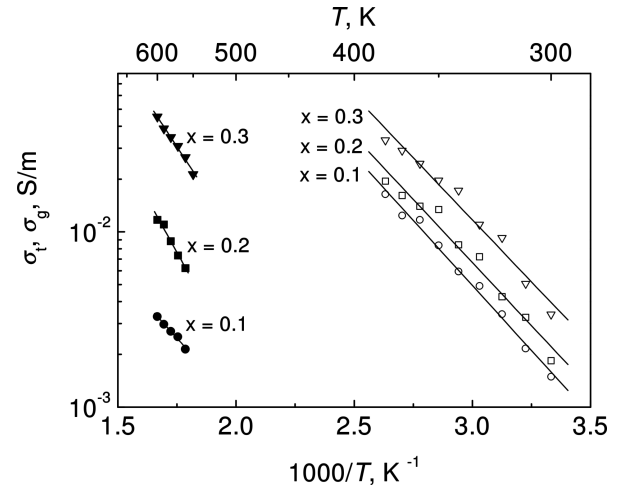


Fig. 4. Temperature dependences of total ($\bullet, \blacksquare, \blacktriangledown$) and grain ($\circ, \square, \triangledown$) conductivities of $\text{Li}_{1+x}\text{Sc}_x\text{Zr}_{2-x}(\text{PO}_4)_3$ ceramics.

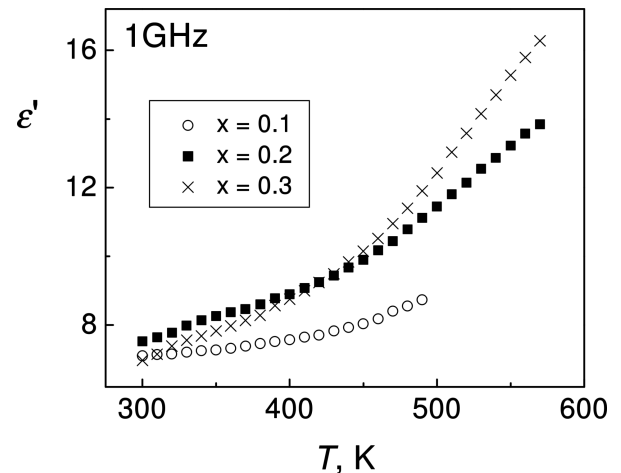


Fig. 5. Temperature dependences of dielectric permittivity of $\text{Li}_{1+x}\text{Sc}_x\text{Zr}_{2-x}(\text{PO}_4)_3$ ceramics.

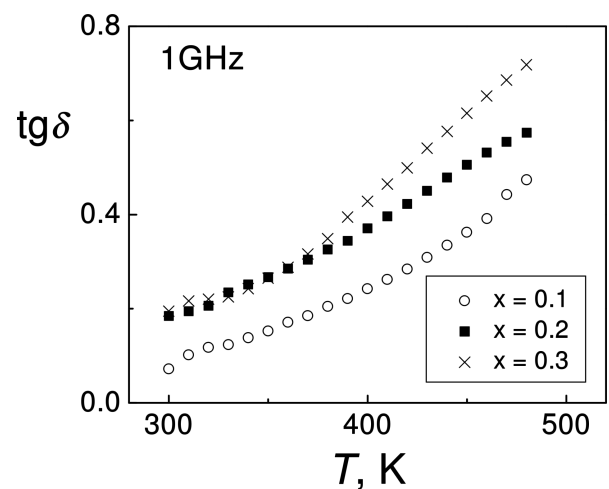


Fig. 6. Temperature dependences of dielectric losses of $\text{Li}_{1+x}\text{Sc}_x\text{Zr}_{2-x}(\text{PO}_4)_3$ ceramics.

$T = 300$ K the real part of complex permittivity with $x = 0.1, 0.2$, and 0.3 were found to be $7.1, 7.5$, and 7.0 respectively. At room temperature the values of dielectric losses of the ceramics with $x = 0.1, 0.2$, and 0.3 were found to be $0.072, 0.18$, and 0.19 respectively. The increase of the values of ϵ' with temperature of the investigated compounds can be caused by the contribution of the migration polarization of lithium ions, lattice vibrations, and electronic polarization. The increase of $\tan \delta$ with temperature is related to the contribution of conductivity in the investigated temperature region.

4. Conclusion

The solid electrolyte $\text{Li}_{1+x}\text{Sc}_x\text{Zr}_{2-x}(\text{PO}_4)_3$ (where $x = 0.1, 0.2, 0.3$) compounds have been synthesized by solid phase reactions and studied by the X-ray powder diffraction. The investigated compounds belong to rhombohedral symmetry (space group $R\bar{3}c$) with $z = 6$ formula units in the lattice. The ceramic of $\text{Li}_{1+x}\text{Sc}_x\text{Zr}_{2-x}(\text{PO}_4)_3$ with $x = 0.1, 0.2$, and 0.3 were sintered at temperature $T = 1643$ K. The ceramic samples were investigated by complex impedance spectroscopy in the frequency range from 10^6 to $1.2 \cdot 10^9$ Hz at the temperatures ranging from 300 to 600 K. Two regions of the impedance dispersion are analysed in terms of transport of the fast Li^+ ions in the grains and grain boundaries of the ceramic samples. The values of σ_t , σ_g , and their activation energies depend on the stoichiometric parameter x . The values of ϵ' at room temperature and 1 GHz frequency are related mainly to the polarization process due to migration of Li^+ ions, lattice vibrations, and electronic polarization.

References

- [1] M. Broussely, J.P. Planckat, G. Rigobert, D. Virey, and G. Sarre, *J. Power Sources* **68**, 8–12 (1997).
- [2] P. Birke, F. Salam, S. Doring, and W. Weppner, *Solid State Ionics* **118**, 149–157 (1999).
- [3] W. Weppner, *Ionics* **5**, 355–359 (1999).
- [4] A. Orliukas, J. Sinius, V. Kazlauskienė, and A. Kežionis, *Mater. Sci.* **8**, 65–67 (2002).
- [5] M.A. Subramanian, R. Subramanian, and A. Clearfield, *Solid State Ionics* **18–19**, 562–569 (1986).
- [6] H. Aono, E. Sugimoto, Y. Sadaoka, N. Imanoka, and G. Adachi, *J. Electrochem. Soc.* **137**, 1023–1027 (1990).
- [7] J.E. Iglesias and C. Pecharrromán, *Solid State Ionics* **112**, 309–318 (1998).
- [8] S. Hamdoune, D. Tranqui, and E.J.L. Schouler, *Solid State Ionics* **18–19**, 587–591 (1986).
- [9] Z.-X. Lin, H.-J. Yu, S.-C. Li, and S.-B. Tian, *Solid State Ionics* **31**, 91–94 (1988).
- [10] B.E. Taylor, A.D. English, and T. Berzins, *Mater. Res. Bull.* **12**, 171–181 (1977).
- [11] F. Sudreau, D. Petit, and J.P. Boilot, *J. Solid State Chem.* **83**, 78–90 (1989).
- [12] M. Catti, S. Stramare, and R. Ibberson, *Solid State Ionics* **123**, 173–180 (1999).
- [13] D. Petit, Ph. Colomban, G. Collin, and J.P. Bailot, *Mater. Res. Bull.* **21**, 365–371 (1986).
- [14] A.F. Orliukas, A. Kežionis, and E. Kazakevicius, *Solid State Ionics* **176**, 2037–2043 (2005).
- [15] *ASTM X-ray Powder Diffraction File*, Data No. 30-777 (JCPDS-ICDD, 1993).
- [16] *Scientific Laboratory Instruments. Apparatus. Chemicals. Table of Periodic Properties of the Elements. Catalog No. S-18806* (E.H. Sargent & Co., 1964), side 2.
- [17] H. Aono, E. Sugimoto, Y. Sadaoka, N. Imanoka, and G. Adachi, *Solid State Ionics* **40–41**, 38–42 (1990).
- [18] R. Sobiestianskas, A. Dindune, Z. Kanepe, J. Ronis, A. Kežionis, E. Kazakevičius, and A. Orliukas, *Mater. Sci. Eng. B* **76**, 184–192 (2000).
- [19] W. Bogusz, J.R. Dygas, F. Krok, A. Kežionis, R. Sobiestianskas, E. Kazakevicius, and A. Orliukas, *Phys. Status Solidi A* **183**, 323–330 (2001).
- [20] M. Cretin and P. Fabry, *J. Eur. Ceram. Soc.* **19**, 2931–2940 (1999).
- [21] M. Gödickemeier, B. Michel, A. Orliukas, P. Bohac, K. Sasaki, L. Gauckler, H. Heinrich, P. Schwander, G. Kostorz, H. Hofmann, and O. Frei, *J. Mater. Res.* **9**, 1228–1240 (1994).

$\text{Li}_{1+x}\text{Sc}_x\text{Zr}_{2-x}(\text{PO}_4)_3$ ($x = 0,1, 0,2, 0,3$) KERAMIKŲ SINTEZĖ, SANDARA IR ELEKTRINĖS SAVYBĖST. Šalkus^a, A. Dindune^b, Z. Kanepe^b, J. Ronis^b, A. Kežionis^a, A.F. Orliukas^a^a Vilniaus universitetas, Vilnius, Lietuva^b Rygos technikos universiteto Neorganinės chemijos institutas, Salaspilis, Latvija**Santrauka**

Kietieji $\text{Li}_{1+x}\text{Sc}_x\text{Zr}_{2-x}(\text{PO}_4)_3$ (čia $x = 0,1, 0,2, 0,3$) elektrolitai buvo sintezuoti kietųjų fazių reakcijų metodu. Jų kristalinė sandara buvo tirta kambario temperatūroje Rentgeno spindulių difrakcijos nuo miltelių metodu. Nustatyta, kad tirtieji junginiai priklauso romboedrinei singonijai (erdvinė simetrijos grupė $R\bar{3}c$), o jų elementariojoje kristalinėje gardelėje yra 6 formuliniai vienetai. Buvo pagamintos tų kietųjų elektrolitų keramikos. Keramikų elektrinės savybės buvo tirtos impedanso spektroskopijos metodu, matuojant jų pilnutinę varžą, kompleksinį laidį ir kompleksinę dielektrinę skvarbą 10^6 – $1,2 \cdot 10^9$ Hz dažnio elektriniuose laukuose

300–600 K temperatūros intervale. Tirtose keramikose pastebimos dvi relaksacinio tipo elektrinių parametrų dispersijos, susijusios su Li^+ jonų pernaša kristalituose ir tarpkristalitinėse terpėse. Didėjant stechiometrijos parametrai x , kristalitinis (σ_g) ir bendrasis (σ_t) laidžiai didėja. Išmatuoti $\text{Li}_{1+x}\text{Sc}_x\text{Zr}_{2-x}(\text{PO}_4)_3$ keramikų dielektrinė skvarba ε' ir dielektriniai nuostoliai $\tan \delta$ priklauso nuo stechiometrijos parametro x . Didėjant temperatūrai, keramikų ε' ir $\tan \delta$ didėja. Keramikų ε' vertę lemia ličio jonų migracinė, joninė tamproji bei elektroninė poliarizacijos. Matuotų kietųjų elektrolitų dielektriniai nuostoliai atsiranda dėl jų joninio laidumo kaitos.